The basal ganglia communicate with the cerebellum

Andreea C. Bostan[a], Richard P. Dum[a], and Peter L. Strick[a,b,1]

[a]Center for the Neural Basis of Cognition, Systems Neuroscience Institute and Department of Neurobiology, University of Pittsburgh School of Medicine, Pittsburgh, PA 15261; and [b]Pittsburgh Veterans Affairs Medical Center, Pittsburgh, PA 15240

The basal ganglia and cerebellum are major subcortical structures that influence not only movement, but putatively also cognition and affect. Both structures receive input from and send output to the cerebral cortex. Thus, the basal ganglia and cerebellum form multisynaptic loops with the cerebral cortex. Basal ganglia and cerebellar loops have been assumed to be anatomically separate and to perform distinct functional operations. We investigated whether there is any direct route for basal ganglia output to influence cerebellar function that is independent of the cerebral cortex. We injected rabies virus (RV) into selected regions of the cerebellar cortex in cebus monkeys and used retrograde transneuronal transport of the virus to determine the origin of multisynaptic inputs to the injection sites. We found that the subthalamic nucleus of the basal ganglia has a substantial disynaptic projection to the cerebellar cortex. This pathway provides a means for both normal and abnormal signals from the basal ganglia to influence cerebellar function. We previously showed that the dentate nucleus of the cerebellum has a disynaptic projection to an input stage of basal ganglia processing, the striatum. Taken together these results provide the anatomical substrate for substantial two-way communication between the basal ganglia and cerebellum. Thus, the two subcortical structures may be linked together to form an integrated functional network.

cerebellar cortex | subthalamic nucleus | virus tracing

The basal ganglia and cerebellum are major subcortical structures that influence not only movement, but putatively also cognition and affect (1, 2). Both structures receive input from and send output to the cerebral cortex. Thus, the basal ganglia and cerebellum form multisynaptic loops with the cerebral cortex. The major interactions between these loops were thought to occur largely at the cortical level (3). Recently, we showed that one of the output nuclei of the cerebellum, the dentate nucleus, has a disynaptic projection to an input stage of basal ganglia processing, the striatum (4). This pathway enables cerebellar output to influence basal ganglia function. Here, we investigated whether a comparable pathway allows basal ganglia output to influence cerebellar function. We injected rabies virus (RV) into regions of the cerebellar cortex in cebus monkeys and used retrograde transneuronal transport of the virus to determine the origin of multisynaptic inputs to the injection sites. Our results indicate that the subthalamic nucleus (STN) of the basal ganglia has substantial disynaptic projections to the cerebellar cortex.

Results

We injected the N2c strain of RV into selected sites within the cerebellar cortex of three cebus monkeys (Fig. 1 and Table S1). RV is transported transneuronally in the retrograde direction in a time-dependent fashion in nonhuman primates (4–8). We set the survival time at 42 h to allow two stages of transport: retrograde transport of RV to first-order neurons that project to the injection site and then, retrograde transneuronal transport of the virus to second-order neurons that make synaptic connections with the first-order neurons. The suitability of the survival time was confirmed by the presence of second-order neurons labeled in cortical layer V, the site of corticopontine neurons (9), and by the absence of third-order neurons labeled in layer III.

Our injections targeted Crus IIp (*n* = 2) and the hemispheric expansion of lobule VIIB (HVIIB) (*n* = 1) (Fig. 2*A*). In all cases we mixed RV with a conventional tracer, the β subunit of cholera toxin (CTb, 0.02%). We used this mixture to facilitate identification of the RV injection site and to label neurons that project directly to it (first-order neurons). After RV-CTb injections into Crus IIp and HVIIB, we found first-order neurons labeled with CTb and RV in regions of the pontine nuclei (Fig. S1) and the inferior olive that are known to project to the injected regions of the cerebellar cortex (10–12). We found second-order neurons labeled with RV in cortical areas and in regions of the parvocellular portion of the red nucleus (Fig. 3*A*) that are known to project to the first-order neurons in the pontine nuclei and the inferior olive (9, 13).

Surprisingly, we also found substantial numbers of second-order neurons labeled with RV in the STN predominantly on the side contralateral to the injection site (Figs. 1, 2*B*, 3, and 4). We counted labeled neurons on every other section through the STN of the two animals illustrated in the figures and found 1,160 second-order neurons in the STN after the Crus IIp injection (AB2) and 923 second-order neurons after the HVIIB injection (AB3).

In all animals, second-order neurons labeled with RV were present throughout the entire rostrocaudal extent of the STN (Figs. 2*B* and 4 *A* and *B*). However, larger numbers of second-order neurons were located in the rostral half of the STN following the Crus IIp injections (AB1 and AB2) (Fig. 4*A* red bars), whereas larger numbers of second-order neurons were located in the caudal half of the STN following the HVIIB injections (AB3) (Fig. 4*A* blue bars). The second-order neurons labeled from Crus IIp and HVIIB injections also differed in their dorsoventral and mediolateral distribution. Second-order neurons projecting to Crus IIp were located more ventromedially in the STN than those projecting to HVIIB (Figs. 2*B* and 4*B*). These observations indicate that there is a disynaptic connection between the STN and the cerebellar cortex and that this connection is topographically organized.

The STN has been subdivided into three functional territories: sensorimotor, associative, and limbic (Fig. 4*C*). These subdivisions are based on STN interconnections with regions of the globus pallidus and the ventral pallidum (14–16). The pattern of inputs from the cerebral cortex to the STN also imposes a functional topography on the STN (Fig. 4*D*). A comparison of our data with these functional subdivisions indicates that most of the STN neurons that project to Crus IIp are located in its associative territory, which receives input from the frontal eye fields and regions of prefrontal cortex. In contrast, most of the STN neurons that project to HVIIB are located in its sensorimotor territory, which receives input from the primary motor cortex and several of the premotor areas in the frontal lobe. Although we have examined only a relatively small
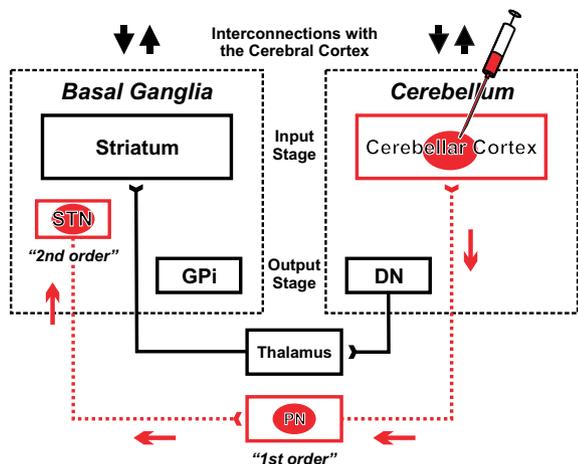
Fig. 1. Experimental paradigm and circuits interconnecting basal ganglia and cerebellum. We injected rabies virus (RV) into regions of the cerebellar hemisphere. The virus went through two stages of transport: retrograde transport to first-order neurons that innervate the injection site and then, retrograde transneuronal transport to second-order neurons that innervate the first-order neurons. The red arrows indicate the direction of virus transport. Previously, we have shown that an output stage of cerebellar processing, the dentate nucleus (DN), has a disynaptic connection with an input stage of basal ganglia processing, the striatum (4). In this experiment, we demonstrate a reciprocal connection from the subthalamic nucleus (STN) to the input stage of cerebellar processing, the cerebellar cortex. These interconnections enable two-way communication between the basal ganglia and cerebellum. Each of these subcortical modules has separate parallel interconnections with the cerebral cortex (up and down black arrows). DN, dentate nucleus; GPi, internal segment of the globus pallidus; PN, pontine nuclei; STN, subthalamic nucleus.

portion of the cerebellar cortex, these results suggest that the STN–cerebellar connection is involved in integrating basal ganglia and cerebellar functions in both motor and nonmotor domains.

The nuclei, which mediate the disynaptic connection between the STN and the cerebellum, remain to be determined. However, the STN is known to project to the nucleus reticularis tegmenti pontis (NRTP) and several basal pontine nuclei (17). As noted above, we observed first-order neurons labeled with CTb and RV in the NRTP and multiple basal pontine nuclei after our tracer injections (Fig. S1). Thus, we view the pontine nuclei as the most likely candidates for mediating the disynaptic connection, but this proposal remains to be tested in future experiments.

Discussion

The STN has been described as the "driving force of the basal ganglia" (18). Our results indicate that this driving force extends well beyond the nuclei of the basal ganglia to the cerebellum. As a consequence, the anatomical substrate exists for both normal and abnormal signals from the STN to influence cerebellar processing. The topographic organization of this disynaptic pathway suggests that STN output could have an impact on cerebellar function during motor and nonmotor behavior. In the following paragraphs we will briefly describe some of the potential implications of this pathway for cerebellar involvement in (*i*) prototypical basal ganglia disorders and (*ii*) reward processing.

Parkinson's disease (PD) and dystonia are traditionally considered to be "basal ganglia disorders." PD is associated with degeneration of a specific set of dopaminergic neurons in the pars compacta of the substantia nigra. Acquired (secondary) dystonia also is often associated with lesions of the basal ganglia (19). Although no overt neurodegeneration has been identified in idiopathic (primary) dystonia, there is evidence for alterations in the basal ganglia in this form of the disorder as well (20). Despite these results, a number of observations have suggested that alterations in cerebellar activity may contribute to the motor symptoms of both PD and dystonia. For example, imaging studies report marked abnormal increases in cerebellar activity in PD patients and in subjects with idiopathic dystonia (20–22). In PD, deep brain stimulation of the STN improves the motor signs and normalizes cerebellar activation (22, 23). In addition, one of the cardinal symptoms
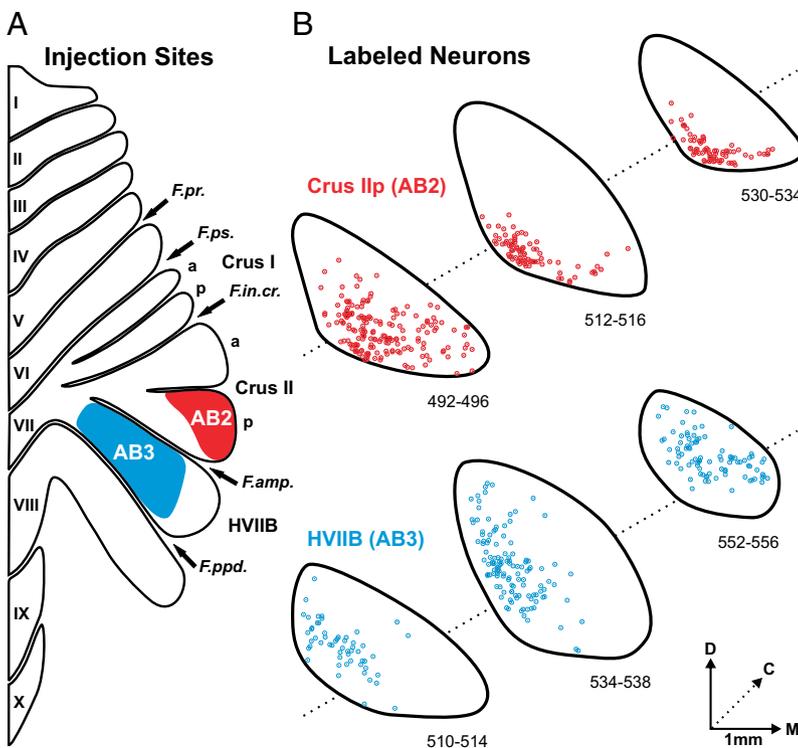
Fig. 2. Injection sites and second-order neurons labeled in STN. (*A*) The injection sites of rabies virus (RV) with cholera toxin subunit β (CTb) are outlined on a flattened map of the cerebellar cortex adapted from ref. 7. The injection in AB2 (red filled area) targeted Crus IIp. The injection site in another animal (AB1, not illustrated) also targeted Crus IIp. In this case the injection site overlapped, but was somewhat less extensive than that of AB2. The injection in AB3 (blue filled area) targeted HVIIB. (*B*) Cross-sections of the STN show the location of second-order neurons labeled by the retrograde transneuronal transport of RV from Crus IIp in AB2 (red dots) and from HVIIB in AB3 (blue dots). Each of the three rostrocaudal levels displayed is spaced ≈1 mm apart. Labeled neurons from three consecutive sections (spaced 100 μm apart) are overlapped at each level. a, anterior; C, caudal; D, dorsal; F.amp., ansoparamedian fissure; F.in.cr., intracrural fissure; F.ppd., prepyramidal fissure; F.pr., primary fissure; F.ps., posterior superior fissure; M, medial; p, posterior.

NEUROSCIENCE

Fig. 3. Second-order neurons in the STN labeled by the retrograde transneuronal transport of RV. (*A*) Chart of a coronal section through the midbrain in one monkey (AB2). Each dot represents a neuron infected with RV. (*B*) Photomicrograph of the boxed area in *A*. Arrows point to examples of second-order neurons labeled with RV. (*C*) Enlargement of the boxed area in *B*. D, dorsal; M, medial; RNpc, parvocellular red nucleus; SNpc, substantia nigra pars compacta; SNr, substantia nigra pars reticulata; ZI, zona incerta.

Fig. 4. Topography of STN projections to the cerebellar hemisphere. (*A*) Histogram of the rostrocaudal distribution of second-order neurons in STN in AB2 (red bars) and AB3 (blue bars). The distance between two consecutive sections represented is 100 μm. Missing bars correspond to missing sections. (*B*) Charts of labeled neurons in AB2 (red dots) and AB3 (blue dots) are overlapped to illustrate the topographic differences in distribution of second-order neurons in STN of the two cases. (*C*) Schematic representation of STN organization, according to the tripartite functional subdivision of the basal ganglia (adapted from ref. 16). (*D*) Schematic summary of the known connections of the STN with areas of the cerebral cortex (based on refs. 31–36). C, caudal; D, dorsal; M, medial.

of PD, tremor at rest, is abolished by stimulating or lesioning the ventral intermediate nucleus of the thalamus, which is a target of cerebellar efferents (24). Similarly, in a mouse model of dystonia, pharmacological stimulation of the cerebellar vermis elicited dystonic postures of the trunk and limbs (25).

The discovery of a disynaptic connection between the basal ganglia and cerebellum provides a unique framework for interpreting these results. It is notable that in both PD and idiopathic dystonia, neural activity in the STN is higher than normal and is characterized by abnormal bursting and oscillatory activity (26). Abnormal signals from the STN to the cerebellar cortex could evoke the increased cerebellar activation that is present in both disorders and alter cerebellothalamocortical input to the cerebral cortex. Further attempts to ameliorate the symptoms of PD and dystonia might benefit by focusing specifically on normalizing activity in the disynaptic pathway from STN to the cerebellum. In fact, part of the effectiveness of deep brain stimulation of the STN might be achieved through this mechanism.

Our findings also provide a potential explanation for the presence of cerebellar activation in imaging studies that were explicitly designed to study the normal functions of the basal ganglia. For example, several imaging studies have examined whether regions of

the basal ganglia and related cortical areas display functional activation consistent with their involvement in "temporal difference" models of reward-related learning (27, 28). It is noteworthy that robust cerebellar activation was present in these experiments along with activation in the dorsal and ventral striatum. The disynaptic connection between the STN and the cerebellum provides an anatomical substrate for reward-related signals in the basal ganglia to influence cerebellar function during learning.

From a computational perspective, the basal ganglia and cerebellum have been viewed as segregated modules that implement different learning algorithms—reinforcement learning in the case

of the basal ganglia and supervised learning in the case of the cerebellum (29, 30). A previous study from our lab demonstrated that an output stage of cerebellar processing, the dentate nucleus, has a disynaptic connection with the input stage of basal ganglia processing, the striatum (4) (Fig. 1). The current report provides evidence for the reciprocal connection. Taken together these results provide the neural basis for substantial two-way communication between the basal ganglia and cerebellum. Thus, the two subcortical structures may be linked together to form an integrated functional network. One might then ask what new computational operations emerge by interconnecting a reinforcement learning module with a supervised learning module.

Methods

Subjects. This report is based on observations from three cebus monkeys (*Cebus apella*, 1.9–2.6 kg, 2 males and 1 female). In each monkey, a mixture of the N2c strain of the RV and a conventional tracer [β subunit of cholera toxin (CTb)] was injected into the cortex of the cerebellar hemisphere. The protocol was approved by the institutional animal care and use committee and the biosafety committee. Biosafety practices conformed to the biosafety level 2 regulations outlined in Biosafety in Microbiological and Biomedical Laboratories (Department of Health and Human Services publication no. 93–8395). Details of the procedures for handling virus and virus-infected animals have been published previously (5).

Experimental Procedures. All surgical procedures were performed under aseptic conditions. The night before surgery, the monkeys were administered dexamethasone (0.5 mg/kg, i.m.). Monkeys were sedated with ketamine (20 mg/kg, i.m.), intubated, and maintained on gas anesthesia (enflurane; 1.5–2.5%). Dexamethasone (0.5 mg/kg, i.m.), glycopyrrolate (0.01 mg/kg, i.m.), and an antibiotic (ceftriaxone; 75 mg/kg, i.m.) were administered at the time of surgery. Respiratory rate, blood oxygen level, body temperature, and sensitivity to noxious stimuli were monitored at regular intervals during the procedure. Each monkey had its head restrained in a Kopf stereotaxic frame (Kopf Instruments). A craniotomy was performed to expose the ventral portions of the occipital cortex and the lateral portion of the posterior cerebellum. With the aid of a surgical microscope, we used a Hamilton syringe (30-gauge needle) to place multiple injection tracks into the cerebellar hemisphere (Crus IIp in animals AB1 and AB2, HVIIB in AB3). We injected small amounts (0.2 μL) of a mixture of RV (4.5×10^9 pfu/mL; provided by M. Schnell) and CTb (0.02%; List Biological Laboratories) at every 0.5 mm along the depth of each injection track (Table S1). The depths of these injections were based on prior structural magnetic resonance images of each cerebellum. When all injections were completed, the cerebellum was covered with artificial dura and the incision was closed in anatomical layers. The monkeys were placed in an isolation chamber and administered an analgesic (buprenorphine; 0.01 mg/kg) and dexamethasone (0.25 mg/kg) every 12 h.

Prior studies have demonstrated that RV is transported exclusively in the retrograde direction in a time-dependent fashion (4–8). The available evidence suggests that the spread of RV is exclusively transsynaptic and that the virus is neither taken up by fibers of passage nor transported between neurons and glia (5). The time to infect first-, second- and third-order neurons depends on the strain of RV and its concentration. The N2c strain used

in the present experiments is transported at a higher transfer rate than other strains used for tracing (e.g., CVS-11). In the current experiments, we set the survival time following the cerebellar injections to 42 h (Fig. 1 and Table S1). This survival time was based on a series of experiments that examined a range of survival times following central injections of the N2c strain (4). A 42-h time period is long enough to allow transport of the virus only to second-order neurons.

At the end of the survival time, the monkeys were deeply anesthetized using ketamine (25 mg/kg, i.p.) followed by pentobarbital sodium (40 mg/kg, i.p.). They were perfused transcardially with 0.1 M phosphate buffer (pH 7.4), followed by 10% buffered formalin, and finally a mixture of 10% buffered formalin and 10% glycerol at 4 °C. The brain and spinal cord were removed from the skull and stored overnight in 10% buffered formalin and 10% glycerol at 4 °C and then placed in 10% buffered formalin and 20% glycerol at 4 °C for 2 weeks. Blocks of tissue (cerebral cortex, brainstem, and cerebellum) were individually frozen and sectioned at 50 μm. Every 10th section was stained with cresyl violet for cytoarchitecture analysis. Brain sections were immunohistochemically reacted according to the avidin-biotin peroxidase method (Vectastain; Vector Laboratories). Alternating sections were reacted with mouse anti-M957 (supplied by A. Wandeler, 1:300) and goat anti-choleragenoid (List Biological Laboratories, 1:10,000) to detect rabies virus or CTb, respectively. Reacted tissue sections were mounted on gelatin-coated glass slides, air dried, and coverslipped.

Data Analysis. Brain sections through the cerebral cortex, brainstem, and the cerebellum were examined for immunostaining using bright field and polarized illumination. Images of selected anatomical structures (Fig. 3 *B* and *C*) were obtained using a digital camera (RT3 monochrome camera, Diagnostic Instruments) coupled to a personal computer. The images were adjusted for contrast, brightness, and intensity using Corel Photopaint. Data were plotted using a computerized plotting system (MD2; Accustage). This system uses optical encoders to measure the *X–Y* movements of the microscope stage and stores the coordinates of section outlines and labeled neurons.

Injection Sites. We used the CTb labeling to identify and reconstruct the injection sites (8). The plotted sections with outlines of the injection site were used to create a flattened map of the cerebellum (following a procedure adapted from ref. 7). Flattened maps of the cerebellar cortex and corresponding injection sites were created for each animal, using custom laboratory software. The injection sites were then outlined on a representative map of a cebus monkey cerebellar cortex (adapted from ref. 7) (Fig. 2*A*).

1. Alexander GE, DeLong MR, Strick PL (1986) Parallel organization of functionally segregated circuits linking basal ganglia and cortex. *Annu Rev Neurosci* 9:357–381.
2. Strick PL, Dum RP, Fiez JA (2009) Cerebellum and nonmotor function. *Annu Rev Neurosci* 32:413–434.
3. Percheron G, François C, Talbi B, Yelnik J, Fénelon G (1996) The primate motor thalamus. *Brain Res Brain Res Rev* 22:93–181.
4. Hoshi E, Tremblay L, Féger J, Carras PL, Strick PL (2005) The cerebellum communicates with the basal ganglia. *Nat Neurosci* 8:1491–1493.
5. Kelly RM, Strick PL (2000) Rabies as a transneuronal tracer of circuits in the central nervous system. *J Neurosci Methods* 103:63–71.
6. Ugolini G (1995) Specificity of rabies virus as a transneuronal tracer of motor networks: Transfer from hypoglossal motoneurons to connected second-order and higher order central nervous system cell groups. *J Comp Neurol* 356:457–480.
7. Kelly RM, Strick PL (2003) Cerebellar loops with motor cortex and prefrontal cortex of a nonhuman primate. *J Neurosci* 23:8432–8444.
8. Prevosto V, Graf W, Ugolini G (2010) Cerebellar inputs to intraparietal cortex areas LIP and MIP: Functional frameworks for adaptive control of eye movements, reaching, and arm/eye/head movement coordination. *Cereb Cortex* 20:214–228.
9. Glickstein M, May JG, 3rd, Mercier BE (1985) Corticopontine projection in the macaque: The distribution of labelled cortical cells after large injections of horseradish peroxidase in the pontine nuclei. *J Comp Neurol* 235:343–359.
10. Brodal P (1979) The pontocerebellar projection in the rhesus monkey: An experimental study with retrograde axonal transport of horseradish peroxidase. *Neuroscience* 4:193–208.
11. Brodal P (1980) The projection from the nucleus reticularis tegmenti pontis to the cerebellum in the rhesus monkey. *Exp Brain Res* 38:29–36.
12. Brodal P, Brodal A (1981) The olivocerebellar projection in the monkey. Experimental studies with the method of retrograde tracing of horseradish peroxidase. *J Comp Neurol* 201:375–393.
13. Strominger NL, Truscott TC, Miller RA, Royce GJ (1979) An autoradiographic study of the rubroolivary tract in the rhesus monkey. *J Comp Neurol* 183:33–45.
14. Parent A, Hazrati LN (1995) Functional anatomy of the basal ganglia. II. The place of subthalamic nucleus and external pallidum in basal ganglia circuitry. *Brain Res Brain Res Rev* 20:128–154.
15. Joel D, Weiner I (1997) The connections of the primate subthalamic nucleus: Indirect pathways and the open-interconnected scheme of basal ganglia-thalamocortical circuitry. *Brain Res Brain Res Rev* 23:62–78.
16. Hamani C, Saint-Cyr JA, Fraser J, Kaplitt M, Lozano AM (2004) The subthalamic nucleus in the context of movement disorders. *Brain* 127:4–20.
17. Giolli RA, et al. (2001) Cortical and subcortical afferents to the nucleus reticularis tegmenti pontis and basal pontine nuclei in the macaque monkey. *Vis Neurosci* 18:725–740.

NEUROSCIENCE

18. Kitai ST, Kita H (1987) *The Basal Ganglia II–Structure and Function: Current Concepts*, eds Carpenter MB, Jayaraman A (Plenum, New York), pp 357–373.

19. Bhatia KP, Marsden CD (1994) The behavioural and motor consequences of focal lesions of the basal ganglia in man. *Brain* 117:859–876.

20. Breakefield XO, et al. (2008) The pathophysiological basis of dystonias. *Nat Rev Neurosci* 9:222–234.

21. Eidelberg D (1998) Functional brain networks in movement disorders. *Curr Opin Neurol* 11:319–326.

22. Payoux P, et al. (2004) Subthalamic nucleus stimulation reduces abnormal motor cortical overactivity in Parkinson disease. *Arch Neurol* 61:1307–1313.

23. Grafton ST, et al. (2006) Normalizing motor-related brain activity: Subthalamic nucleus stimulation in Parkinson disease. *Neurology* 66:1192–1199.

24. Benabid AL, et al. (1991) Long-term suppression of tremor by chronic stimulation of the ventral intermediate thalamic nucleus. *Lancet* 337:403–406.

25. Pizoli CE, Jinnah HA, Billingsley ML, Hess EJ (2002) Abnormal cerebellar signaling induces dystonia in mice. *J Neurosci* 22:7825–7833.

26. Schrock LE, Ostrem JL, Turner RS, Shimamoto SA, Starr PA (2009) The subthalamic nucleus in primary dystonia: Single-unit discharge characteristics. *J Neurophysiol* 102:3740–3752.

27. O'Doherty JP, Dayan P, Friston K, Critchley H, Dolan RJ (2003) Temporal difference models and reward-related learning in the human brain. *Neuron* 38:329–337.

28. Seymour B, et al. (2004) Temporal difference models describe higher-order learning in humans. *Nature* 429:664–667.

29. Doya K (2000) Complementary roles of basal ganglia and cerebellum in learning and motor control. *Curr Opin Neurobiol* 10:732–739.

30. Houk JC (2005) Agents of the mind. *Biol Cybern* 92:427–437.

31. Monakow KH, Akert K, Künzle H (1978) Projections of the precentral motor cortex and other cortical areas of the frontal lobe to the subthalamic nucleus in the monkey. *Exp Brain Res* 33:395–403.

32. Stanton GB, Goldberg ME, Bruce CJ (1988) Frontal eye field efferents in the macaque monkey: I. Subcortical pathways and topography of striatal and thalamic terminal fields. *J Comp Neurol* 271:473–492.

33. Nambu A, Takada M, Inase M, Tokuno H (1996) Dual somatotopical representations in the primate subthalamic nucleus: Evidence for ordered but reversed body-map transformations from the primary motor cortex and the supplementary motor area. *J Neurosci* 16:2671–2683.

34. Nambu A, Tokuno H, Inase M, Takada M (1997) Corticosubthalamic input zones from forelimb representations of the dorsal and ventral divisions of the premotor cortex in the macaque monkey: Comparison with the input zones from the primary motor cortex and the supplementary motor area. *Neurosci Lett* 239:13–16.

35. Inase M, Tokuno H, Nambu A, Akazawa T, Takada M (1999) Corticostriatal and corticosubthalamic input zones from the presupplementary motor area in the macaque monkey: Comparison with the input zones from the supplementary motor area. *Brain Res* 833:191–201.

36. Kelly RM, Strick PL (2004) Macro-architecture of basal ganglia loops with the cerebral cortex: Use of rabies virus to reveal multisynaptic circuits. *Prog Brain Res* 143:449–459.